Math 994-002: Applied and Computational Harmonic Analysis, MSU, Spring 2020

Lecture 12: Real Wavelets

February 18, 2020

Lecturer: Matthew Hirn

4.4.3 Real Wavelets

Section 4.3.1 of A Wavelet Tour of Signal Processing.

We now shift our focus to real wavelets. As we shall see, real valued wavelets are good for measuring sharp signal transitions, and in particular measuring the the regularity of $f(t)$ at a specific point $t = u$. Indeed, since $\int \psi = 0$, the wavelet transform $Wf(u,s) = \langle f, \psi_{u,s} \rangle$ measures the variation of f in a neighborhood of u proportional s. "Zooming in" on these variations will allow us to measure the regularity of f at u.

For now we show that like the analytic wavelet transform, the real wavelet transform is invertible and preserves the energy of f. We collect these results in the next theorem.

Theorem 4.7. *Let $\psi \in \mathbf{L}^1(\mathbb{R}) \cap \mathbf{L}^2(\mathbb{R})$ be a real function such that*

$$C_\psi = \int_0^{+\infty} \frac{|\widehat{\psi}(\omega)|^2}{\omega} \, d\omega < +\infty$$

Then, for any $f \in \mathbf{L}^2(\mathbb{R})$,

$$f(t) = \frac{1}{C_\psi} \int_0^{+\infty} \int_{\mathbb{R}} Wf(u,s) \frac{1}{\sqrt{s}} \psi\left(\frac{t-u}{s}\right) du \, \frac{ds}{s^2}$$

and

$$\|f\|_2^2 = \frac{1}{C_\psi} \int_0^{+\infty} \int_{\mathbb{R}} |Wf(u,s)|^2 \, du \, \frac{ds}{s^2}$$

The proof is nearly identical to the proof of Theorem 4.6, and so is omitted. An example of a real valued wavelet, which we shall use later and which also satisfies the conditions of Theorem 4.7, is the so called "Mexican hat wavelet." The Mexican hat wavelet is the second derivative of a suitably normalized Gaussian function $g_\sigma(t)$ with mean zero and standard deviation σ:

$$\psi(t) = g_\sigma''(t) = \frac{2}{\pi^{1/4}\sqrt{3\sigma}} \left(\frac{t^2}{\sigma^2} - 1\right) e^{-t^2/2\sigma^2} \tag{30}$$

The Fourier transform of $\psi(t)$ is

$$\widehat{\psi}(\omega) = -\omega^2 \widehat{g}_\sigma(\omega) = -\frac{\sqrt{8}\sigma^{5/2}\pi^{1/4}}{\sqrt{3}} \omega^2 e^{-\sigma^2\omega^2/2}$$

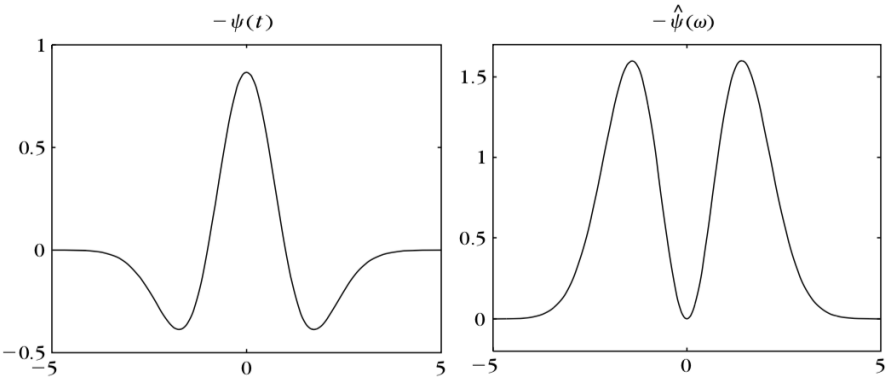

Figure 18: Mexican hat wavelet for $\sigma = 1$ and its Fourier transform.

Figure 18 plots the Mexican hat wavelet and its Fourier transform.

Figure 19 computes the wavelet transform of the signal from Figure 13 using the Mexican hat wavelet. The maximum scale is smaller than one because the support of $f(t)$ is limited to $t \in [0, 1]$. In all numerical calculations, including this one, the minimum scale is limited by the sampling interval of the discretized signal due to aliasing effects. When the scale decreases, the wavelet transform $Wf(u, s)$ has a rapid decay to zero in the regions where the signal is regular. Isolated singularities create cones of large amplitude wavelet coefficients that converge to the locations of the isolated singularities, as on the left hand side of the signal. The right hand side of the signal is singular almost everywhere. If this part can be modeled as a random process or multifractal, then under certain assumptions the distribution of singularities can be estimated from $Wf(u, s)$, which can characterize the underlying signal generation process.

In numerical applications, both the minimum and maximum scale are limited. We now examine the wavelet transform when we compute $Wf(u, s)$ only for $s < s_0$. In this case we lose the low frequency components of $f(t)$, since the supports of $\overline{\psi}_s(\omega) = \sqrt{s}\widehat{\psi}^*(s\omega)$ as $s \to +\infty$ collapse in around $\omega = 0$; see Figure 20 for an illustration.

In order to recover this lost low frequency information, we introduce a single *scaling function* ϕ that is an aggregation of all wavelets at scales larger than one. The modulus of its Fourier transform is defined as:

$$|\widehat{\phi}(\omega)|^2 = \int_1^{+\infty} |\widehat{\psi}(s\omega)|^2 \frac{ds}{s} = \int_\omega^{+\infty} \frac{|\widehat{\psi}(\xi)|^2}{\xi} d\xi \tag{31}$$

The complex phase of $\widehat{\phi}(\omega)$ can be arbitrarily chosen; in particular we can set it to zero so that ϕ is real valued. One can verify that $\|\phi\|_2 = 1$. The definition of $\widehat{\phi}(\omega)$ and the admissibility condition yields:

$$|\widehat{\phi}(\omega)|^2 \leq |\widehat{\phi}(0)|^2 = \lim_{\xi \to 0} |\widehat{\phi}(\xi)|^2 = C_\psi, \quad \forall\, \omega \in \mathbb{R}$$

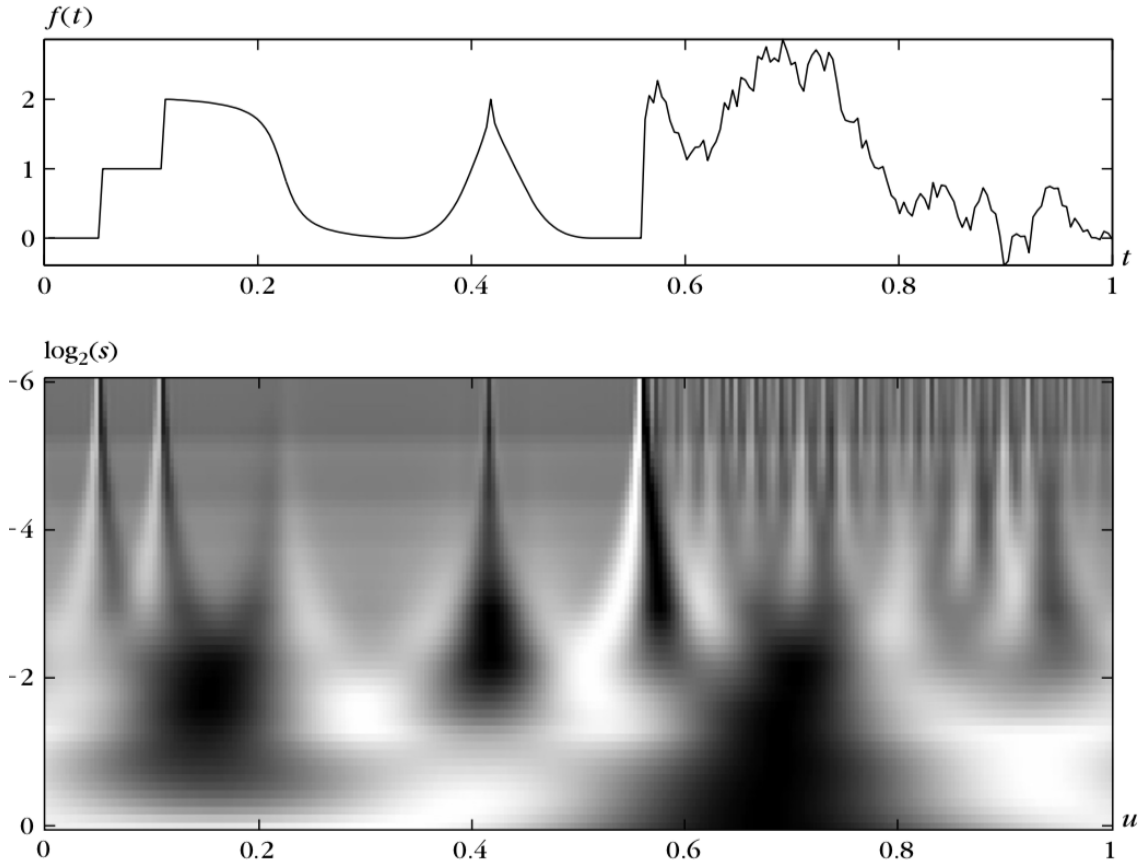

Figure 19: Real wavelet transform $Wf(u,s)$ computed with a Mexcian hat wavelet. The vertical axis represents $\log_2 s$, Black, gray and white points correspond, respectively, to positive, zero, and negative wavelet coefficients.

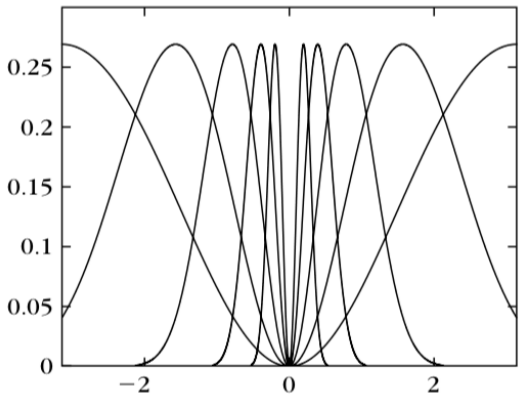

Figure 20: Scaled Fourier transform $|\widehat{\psi}(2^j\omega)|^2$ for $1 \leq j \leq 5$ and $\omega \in [-\pi, \pi]$. Notice the gap around $\omega = 0$ due to the limitation of the largest scale $s = 2^5$.

Denote by $\phi_s(t)$ the scaling of $\phi(t)$ by s:

$$\phi_s(t) = \frac{1}{\sqrt{s}}\phi\left(\frac{t}{s}\right), \quad \overline{\phi}_s(t) = \phi_s^*(-t)$$

The low frequency approximation of f at scale s is

$$Lf(u,s) = f * \overline{\phi}_s(u)$$

In this case, the wavelet inversion formula becomes:

$$f(t) = \frac{1}{C_\psi}\int_0^{s_0} Wf(\cdot,s) * \psi_s(t)\,\frac{ds}{s^2} + \frac{1}{C_\psi s_0} Lf(\cdot,s_0) * \phi_{s_0}(t) \tag{32}$$

For the Mexican hat wavelet defined in (30), the Fourier transform of the scaling function is:

$$\widehat{\phi}(\omega) = \frac{2\sigma^{5/2}\pi^{1/4}}{\sqrt{3}}\sqrt{\omega^2 + \frac{1}{\sigma^2}}e^{-\sigma^2\omega^2/2}$$

See Figure 21 for a plot.

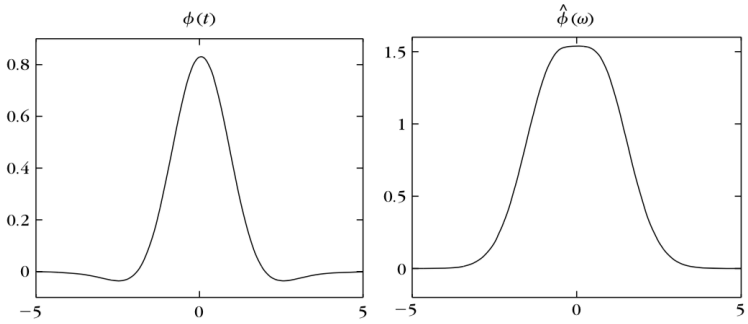

Figure 21: Scaling function associated to a Mexican hat wavelet and its Fourier transform.

Exercise 41. Read Section 4.5 of *A Wavelet Tour of Signal Processing*.

Exercise 42. Let ϕ be the scaling function defined by (31). Prove that $\|\phi\|_2 = 1$.

Exercise 43. Prove the reconstruction formula given in (32), which can be rewritten as:

$$f(t) = \frac{1}{C_\psi}\int_0^{s_0} f * \overline{\psi}_s * \psi_s(t)\,\frac{ds}{s^2} + \frac{1}{C_\psi s_0} f * \overline{\phi}_{s_0} * \phi_{s_0}(t)$$

Exercise 44. [20 points] Implement the real wavelet transform $Wf(u,s)$ using the Mexican hat wavelet. Write down a signal $f(t)$ similar to the one from Figure 13 (does not have to be exactly the same!) and compute $Wf(u,s)$ numerically. Turn in a plot of your signal and a plot of $Wf(u,s)$, as in Figure 19.

5 Wavelet Zoom

Chapter 6 of A Wavelet Tour of Signal Processing [1].

Wavelet transforms can zoom in and characterize the regularity of a function $f(t)$ at individual points $t = v$. We show how in this section.

5.1 Lipschitz Regularity

Section 6.1 of A Wavelet Tour of Signal Processing

5.1.1 Lipschitz Definition and Fourier Analysis

Section 6.1.1 of A Wavelet Tour of Signal Processing

We begin by defining the spaces $\dot{\mathbf{C}}^\alpha(\mathbb{R})$ and $\mathbf{C}^\alpha(\mathbb{R})$ for any $\alpha > 0$, $\alpha \notin \mathbb{Z}$. Let $0 < \alpha < 1$. Define the modulus of continuity of $f(t)$, $\omega_f(h)$, as:

$$\omega_f(h) = \sup\{|f(t) - f(u)| : |t - u| \leq h\}\,.$$

The space $\dot{\mathbf{C}}^\alpha(\mathbb{R})$, for $0 < \alpha < 1$, consists of those functions for which

$$\forall\, h > 0\,, \quad \omega_f(h) \leq K_f h^\alpha$$

Another way of writing this condition is:

$$\forall\, (t, u) \in \mathbb{R}^2\,, \quad |f(t) - f(u)| \leq K_f |t - u|^\alpha$$

We thus see that $\dot{\mathbf{C}}^\alpha(\mathbb{R})$ consists of those functions that satisfy a type of global Lipschitz condition; they are called α-Hölder functions. The space $\mathbf{C}^\alpha(\mathbb{R})$ contains all those functions in $\dot{\mathbf{C}}^\alpha(\mathbb{R})$ that are also bounded, i.e.,

$$\mathbf{C}^\alpha(\mathbb{R}) = \dot{\mathbf{C}}^\alpha(\mathbb{R}) \cap \mathbf{L}^\infty(\mathbb{R})$$

These definitions are extended to arbitrary $\alpha > 0$, $\alpha \notin \mathbb{Z}$, in the following way. Let $n < \alpha < n + 1$ for some $n \in \mathbb{N}$. Then

$$f \in \dot{\mathbf{C}}^\alpha(\mathbb{R}) \quad \Longleftrightarrow \quad f \in \mathbf{C}^n(\mathbb{R}) \text{ and } f^{(n)} \in \dot{\mathbf{C}}^{\alpha - n}(\mathbb{R})$$

where $\dot{\mathbf{C}}^{\alpha-n}(\mathbb{R})$ is defined as above since $0 < \alpha - n < 1$. Similarly,

$$f \in \mathbf{C}^\alpha(\mathbb{R}) \quad \Longleftrightarrow \quad f \in \mathbf{C}^n(\mathbb{R}) \text{ and } f^{(k)} \in \mathbf{C}^{\alpha - n}(\mathbb{R}) \;\; \forall\, k \leq n$$

We can link these definitions to Taylor's theorem. Suppose that $f \in \dot{\mathbf{C}}^\alpha(\mathbb{R})$ for $n < \alpha < n+1$. Let $v \in \mathbb{R}$ and let $J_v f(t)$ be the *jet* of f at v, which is the n-degree Taylor polynomial of f around v:

$$J_v f(t) = \sum_{k=0}^{n} \frac{f^{(k)}(v)}{k!} (t - v)^k$$

Denote the residual by $R_v f(t)$, i.e.,

$$R_v f(t) = f(t) - J_v f(t)$$

Then using Taylor's theorem and the fact that $f \in \dot{\mathbf{C}}^\alpha(\mathbb{R})$,

$$|R_v f(t)| \leq K|t-v|^\alpha$$

Conversely, suppose that $f(t)$ is a continuous function for which there exists a universal constant K and such that for each $v \in \mathbb{R}$, there exists a polynomial $p_v(t)$ of degree at most n such that

$$|f(t) - p_v(t)| \leq K|t-v|^\alpha$$

Then $f \in \dot{\mathbf{C}}^\alpha(\mathbb{R})$.

We can use this link with Taylor's theorem to define notions of local regularity rather than global regularity. In particular, a function $f(t)$ is pointwise Lipschitz $\alpha > 0$ at $v \in \mathbb{R}$ if there exists $K_v > 0$ and a polynomial $p_v(t)$ of degree $n = \lfloor \alpha \rfloor$ such that

$$|f(t) - p_v(t)| \leq K_v|t-v|^\alpha \tag{33}$$

Furthermore, a function f is uniformly Lipschitz α over an interval $[a,b]$ if it satisfies (33) for all $v \in [a,b]$ with a constant K that is independent of v.

Remark 5.1. At each $v \in \mathbb{R}$ the polynomial $p_v(t)$ is unique. Additionally, if f is $n = \lfloor \alpha \rfloor$ times continuously differentiable in a neighborhood of v, then $p_v(t) = J_v f(t)$.

Remark 5.2. A function that is bounded but discontinuous at v is said to Lipschitz $\alpha = 0$ at v. If $\alpha < 1$ at v, then f is not differentiable at v and α characterizes the type of singularity.

References

[1] Stéphane Mallat. *A Wavelet Tour of Signal Processing, Third Edition: The Sparse Way*. Academic Press, 3rd edition, 2008.

[2] Elias M. Stein and Rami Shakarchi. *Fourier Analysis: An Introduction*. Princeton Lectures in Analysis. Princeton University Press, 2003.

[3] John J. Benedetto and Matthew Dellatorre. Uncertainty principles and weighted norm inequalities. *Contemporary Mathematics*, 693:55–78, 2017.

[4] Yves Meyer. *Wavelets and Operators*, volume 1. Cambridge University Press, 1993.

[5] Karlheinz Gröchenig. *Foundations of Time Frequency Analysis*. Springer Birkhäuser, 2001.